

8-1-2019

Optoelectronic properties of methyl-terminated germanane

Clément Livache

Sorbonne Université

Bradley J. Ryan


Iowa State University, bryan@iastate.edu

Utkarsh Ramesh

Iowa State University, uramesh@iastate.edu

See next page for additional authors

Follow this and additional works at: https://lib.dr.iastate.edu/cbe_pubs

 Part of the [Atomic, Molecular and Optical Physics Commons](#), [Chemical Engineering Commons](#), and the [Engineering Physics Commons](#)

The complete bibliographic information for this item can be found at https://lib.dr.iastate.edu/cbe_pubs/384. For information on how to cite this item, please visit <http://lib.dr.iastate.edu/howtocite.html>.

This Article is brought to you for free and open access by the Chemical and Biological Engineering at Iowa State University Digital Repository. It has been accepted for inclusion in Chemical and Biological Engineering Publications by an authorized administrator of Iowa State University Digital Repository. For more information, please contact digirep@iastate.edu.

Optoelectronic properties of methyl-terminated germanane

Abstract

Germanane is a two-dimensional, strongly confined form of germanium. It presents an interesting combination of (i) ease of integration with CMOS technology, (ii) low toxicity, and (iii) electronic confinement which transforms the indirect bandgap of the bulk material into a direct bandgap featuring photoluminescence. However, the optoelectronic properties of this material remain far less investigated than its structural properties. Here, we investigate the photoluminescence and transport properties of arrays of methyl-terminated germanane flakes. The photoluminescence appears to have two contributions, one from the band edge and the other from trap states. The dynamics of the exciton appear to be in the range of 1–100 ns. Conduction in this material appears to be p-type, while the photoconduction time response can be made as short as 100 μ s.

Disciplines

Atomic, Molecular and Optical Physics | Chemical Engineering | Engineering Physics

Comments

This article is published as Livache, Clément, Bradley J. Ryan, Utkarsh Ramesh, Violette Steinmetz, Charlie Gréboval, Audrey Chu, Thibault Brule, Sandrine Ithurria, Geoffrey Prévot, Thierry Barisien, Abdelkarim Ouerghi, Matthew G. Panthani, and Emmanuel Lhuillier. "Optoelectronic properties of methyl-terminated germanane." *Applied Physics Letters* 115, no. 5 (2019): 052106. DOI: [10.1063/1.5111011](https://doi.org/10.1063/1.5111011). Posted with permission.










Authors

Clément Livache, Bradley J. Ryan, Utkarsh Ramesh, Violette Steinmetz, Charlie Gréboval, Audrey Chu, Thibault Brule, Sandrine Ithurria, Geoffrey Prévot, Thierry Barisien, Abdelkarim Ouerghi, Matthew G. Panthani, and Emmanuel Lhuillier

Optoelectronic properties of methyl-terminated germanane

Cite as: Appl. Phys. Lett. **115**, 052106 (2019); <https://doi.org/10.1063/1.5111011>

Submitted: 22 May 2019 . Accepted: 08 July 2019 . Published Online: 01 August 2019

Clément Livache , Bradley J. Ryan, Utkarsh Ramesh, Violette Steinmetz , Charlie Gréboval , Audrey Chu , Thibault Brule, Sandrine Ithurria , Geoffroy Prévot, Thierry Barisien , Abdelkarim Ouerghi , Matthew G. Panthani , and Emmanuel Lhuillier 



View Online



Export Citation



CrossMark

ARTICLES YOU MAY BE INTERESTED IN

[Transient dielectric functions of Ge, Si, and InP from femtosecond pump-probe ellipsometry](#)
Applied Physics Letters **115**, 052105 (2019); <https://doi.org/10.1063/1.5109927>

[Evidence for a narrow band gap phase in 1T' WS₂ nanosheet](#)
Applied Physics Letters **115**, 032102 (2019); <https://doi.org/10.1063/1.5091997>

[Phase and amplitude modulation with acoustic holograms](#)
Applied Physics Letters **115**, 053701 (2019); <https://doi.org/10.1063/1.5110673>



**THE WORLD'S RESOURCE FOR
VARIABLE TEMPERATURE
SOLID STATE CHARACTERIZATION**



Optoelectronic properties of methyl-terminated germanane

Cite as: Appl. Phys. Lett. **115**, 052106 (2019); doi: [10.1063/1.5111011](https://doi.org/10.1063/1.5111011)

Submitted: 22 May 2019 · Accepted: 8 July 2019 ·

Published Online: 1 August 2019



View Online



Export Citation



CrossMark

Clément Livache,^{1,2} Bradley J. Ryan,³ Utkarsh Ramesh,³ Violette Steinmetz,¹ Charlie Gréboval,¹ Audrey Chu,¹ Thibault Brule,⁴ Sandrine Ithurria,² Geoffroy Prévot,¹ Thierry Barisien,¹ Abdelkarim Ouerghi,⁵ Matthew C. Panthani,³ and Emmanuel Lhuillier^{1,a)}

AFFILIATIONS

¹Sorbonne Université, CNRS, Institut des NanoSciences de Paris, 4 place Jussieu, 75005 Paris, France

²Laboratoire de Physique et d'Etude des Matériaux, ESPCI-Paris, PSL Research University, Sorbonne Université Univ Paris 06, CNRS UMR 8213, 10 rue Vauquelin, 75005 Paris, France

³Department of Chemical and Biological Engineering, Iowa State University, Ames, Iowa 50011, USA

⁴HORIBA Scientific, HORIBA France S.A.S., Avenue de la Vauve, Passage Jobin Yvon, 91120 Palaiseau, France

⁵Centre de Nanosciences et de Nanotechnologies, CNRS, University of Paris-Sud, Université Paris-Saclay, C2N, Palaiseau 91460, France

^{a)}Author to whom correspondence should be addressed: el@insp.upmc.fr

ABSTRACT

Germanane is a two-dimensional, strongly confined form of germanium. It presents an interesting combination of (i) ease of integration with CMOS technology, (ii) low toxicity, and (iii) electronic confinement which transforms the indirect bandgap of the bulk material into a direct bandgap featuring photoluminescence. However, the optoelectronic properties of this material remain far less investigated than its structural properties. Here, we investigate the photoluminescence and transport properties of arrays of methyl-terminated germanane flakes. The photoluminescence appears to have two contributions, one from the band edge and the other from trap states. The dynamics of the exciton appear to be in the range of 1–100 ns. Conduction in this material appears to be p-type, while the photoconduction time response can be made as short as 100 μ s.

Published under license by AIP Publishing. <https://doi.org/10.1063/1.5111011>

Nanocrystals have raised substantial interest over the past few years owing to their broadly tunable band edge energy, ranging from the ultraviolet to terahertz spectral regions.^{1,2} Nanocrystals are now commonly used as green light-emitters for display technologies³ or as chlorophyll-optimized down-converters for agricultural lighting. In all these applications, nanocrystals are optically pumped. More advanced applications such as light-emitting diodes (LEDs) or photodetectors⁴ will require films of nanocrystals with suitable transport properties.

Currently, most nanocrystals are based on II–VI and III–V compound semiconductors that possess optical properties in the visible range but contain toxic elements and are difficult to integrate with CMOS technology.⁵ In this sense, nanocrystals made from Group IV compounds are of utmost interest. However, Si^{6,7} and Ge^{8,9} nanocrystals have been far less investigated than other materials such as CdSe and PbS, in particular, due to their sensibility to oxidation.

Beyond these 0D quantum dots, 2D forms of Ge and Si, analogous to graphene, have also generated strong interest in recent years.

Atomically thin sheets of Si and Ge (known as silicene¹⁰ and germanene,¹¹ respectively) have been proposed as alternatives to graphene; however, their feasibility and stability remain controversial.¹² In addition, the bandgap of silicene and germanene is expected to be very narrow,¹³ which make them poor candidates for optoelectronic applications in spite of their low effective masses induced by Dirac cones. In addition and in contrast to graphene, silicene and germanium cannot be separated from their substrate, which makes their device integration even more challenging. It is nevertheless possible to grow 2D sheets of Si and Ge terminated by either hydrogen or methyl groups.^{14–18} These forms of weakly coupled Si and Ge 2D-flakes are called silicane and germanane,^{19–21} and they present a strong confinement leading to a bandgap (1.8 eV for germanane) compatible with electronic and optical applications in the visible region. In addition, their effective masses are expected to be small, which could lead to high carrier mobilities.²² While the electronic structure²³ and structural properties^{22,24} of these materials have been widely investigated,

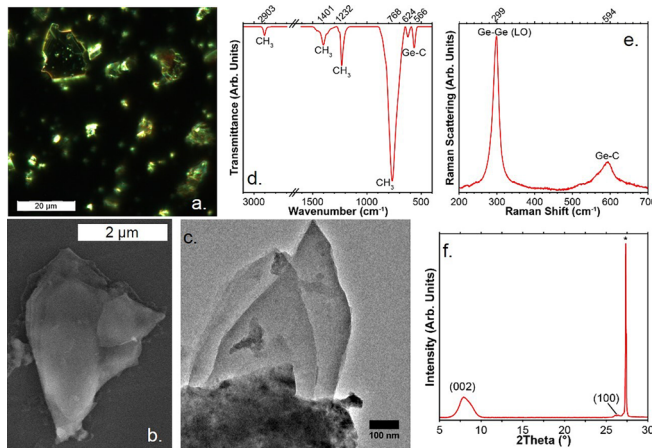


FIG. 1. Dark-field optical (a), scanning electron (b), and transmission electron (c) microscopy images of the methyl-terminated germanane flakes. FTIR (d) and Raman (e) spectra of methyl-terminated germanane powder. (f) Powder X-ray diffraction pattern of methyl-terminated germanane; the narrow peak highlighted with an "asterisk" corresponds to bulk Ge.

especially by the Goldberger group,¹⁴ device integration remains limited.^{25–27} Here, we investigate the optoelectronic properties of methyl-terminated germanane. We unveil their transport and spectroscopic properties which will be of utmost interest for future design of devices based on germanane.

We synthesized methyl-terminated germanane flakes by modifying a procedure reported by Jiang *et al.*,¹⁴ see the [supplementary material](#) for details. The obtained flakes have large lateral dimensions reaching several microns, as revealed by microscopy images in [Figs. 1\(a\)–1\(c\)](#). These germanane flakes are composed of stacks of individual layers (20–50 nm in thickness typically) of methyl-terminated germanane, as revealed by the TEM image, see [Fig. 1\(c\)](#). Fourier-transform infrared (FTIR) spectroscopy confirms the presence of

methyl termination, with vibrational modes arising from C-H and Ge-C bonds, see [Fig. 1\(d\)](#). The Raman spectrum [see [Fig. 1\(e\)](#)] reveals a main contribution appearing at 299 cm^{-1} which is associated with the E_{2g} mode.^{21,28} A second contribution arising from the methyl functionalization appears at 594 cm^{-1} . The X-ray diffraction^{15,18,29} [[Fig. 1\(f\)](#)], in particular, reveals a peak around $2\theta \approx 7.9^\circ$, which, along with Raman and Fourier transform infrared spectroscopy, confirms that the sample contains Ge sheets that are terminated with $-\text{CH}_3$ groups.¹⁵ From Bragg's law, the periodicity of the material is found to be $\approx 1.1\text{ nm}$, corresponding to an interplanar distance of 0.55 nm .

Key interest for this confined form of germanane is the presence of luminescence in the visible range; this is in contrast to the bulk material which presents no luminescence due to the indirect nature of its bandgap. As such, methyl-terminated germanane is a very promising candidate for the fabrication of light-emitting diodes (LEDs). Indeed, current organic and nanocrystal-based LEDs suffer from low light extraction, which limits their conversion efficiency to 20%. This limitation is the result of isotropic emission of photons, which makes that most emitted light is lost due to total internal reflections. Here, due to its 2D geometry, germanane is expected to have anisotropic emission which may improve light extraction.³⁰ The photoluminescence (PL) peak of germanane appears around 700 nm (1.8 eV) around room temperature, see [Fig. 2\(a\)](#).

The full width at half maximum (FWHM) of the PL is $\approx 200\text{ meV}$. Analysis of the temperature dependence of the PL reveals that, with decreasing temperature, the PL intensity increases [[Figs. 2\(e\)](#) and [S1](#)] and broadens [[Figs. 2\(f\)](#) and [S2](#)]. At high temperatures ($>200\text{ K}$), the ensemble PL signal is well fitted by a single Gaussian distribution [see [Fig. S1\(b\)](#)]; the energy of the transition appears at 1.8 eV , which corresponds to the predicted transition for the 2H phase of germanane.¹⁹ PL measurements on a single flake at (250 K) reveals a PL signal with a similar linewidth, see [Fig. 2\(c\)](#). This suggests that the PL linewidth is the result of a homogeneous broadening. At low temperatures, a second contribution appears in the PL signal, see [Fig. 2\(b\)](#), and is responsible for the observed broadening of the PL

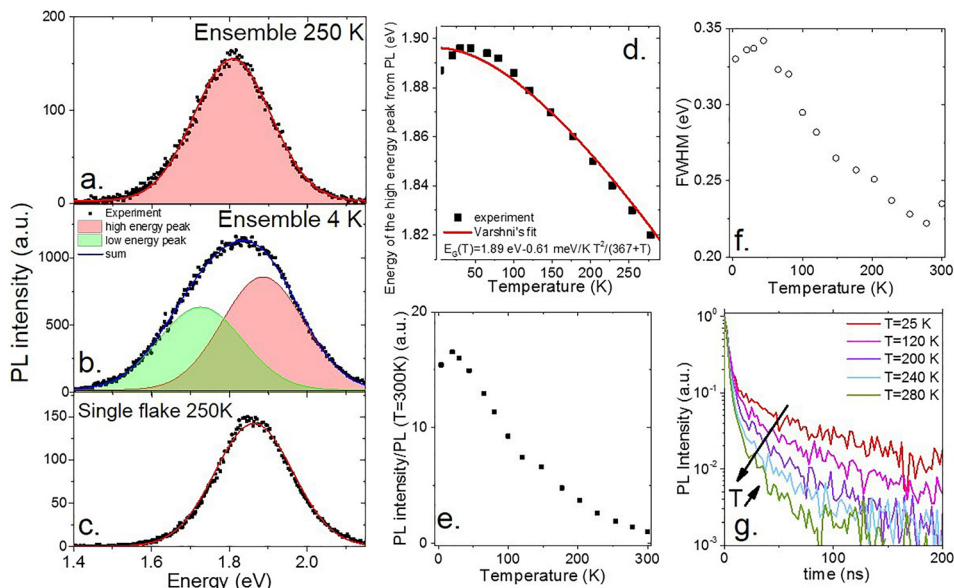


FIG. 2. Photoluminescence (PL) spectra of methyl-terminated germanane flakes: ensemble measurement at 250 K (a), ensemble measurement at 4 K (b), and (c) single flake measurement at 250 K [In all cases, experimental data are points and full curves are Gaussian (or two Gaussian sum) fit.] (d) Temperature dependence of the energy of the low energy peak and its Varshni's fit. (e) PL intensity as a function of temperature for a film of methyl-terminated germanane flakes. (f) Full width at half maximum (FWHM) of the PL signal as a function of temperature for a film of methyl-terminated germanane flakes. (g) Time resolved PL, integrated over the whole spectrum, for a film of methyl-terminated germanane flakes at various temperatures. The arrow shows the trend for the carrier decay as temperature is increased.

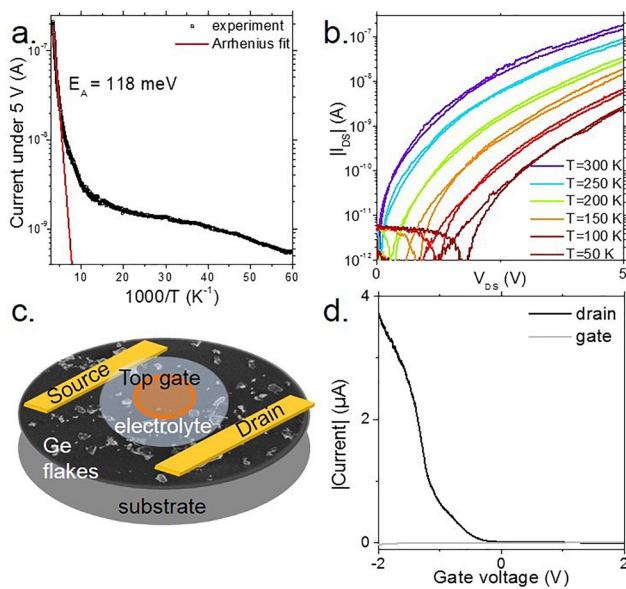


FIG. 3. (a) Diagram of an electrolyte gated field effect transistor, in which the channel is made of a dense film of methyl-terminated germanane flakes. (b) IV curve for a thin film of methyl-terminated germanane flakes at various temperatures. (c) Current as a function of temperature for a thin film of methyl-terminated germanane flakes at various temperatures under +5 V bias. (d) Transfer curve (drain and gate current as a function of the applied gate bias) for an electrolyte gated field effect transistor in which the channel is made of a dense film of methyl-terminated germanane flakes at room temperature. The drain source bias is set at -100 mV.

signal. Since the signal appears at an energy lower than the bandgap value, it is attributed to trap states. Note that depending on the relative weight of the two contributions, the PL peak may sometimes appears at lower energy in the literature.¹⁵

Fitting the high energy contribution (i.e., at the band edge) of the PL with a Varshni's expression, $E_G(T) = E_G(T = 0 \text{ K}) - \frac{A \times T^2}{T + \theta}$, allows for the determination of the temperature dependence of the bandgap with $A = 610 \text{ } \mu\text{eV/K}$ and the phonon temperature $\theta = 367 \text{ K}$. For the sake of comparison, the value of phonon temperature³¹ has been found to be 374 K in the bulk, while the temperature dependence of the bandgap is slightly lower at $460 \text{ } \mu\text{eV/K}$.

Time-resolved PL [Figs. 2(g) and S3] reveals multiexponential behavior. At room temperature, three characteristic lifetimes can be extracted: 2 ns , 20 ns , and 100 ns . After $2 \text{ } \mu\text{s}$, the PL signal has fully

decayed. We observe that the lifetime increases as temperature decreases. This is correlated with increased trap emission at low temperatures, suggesting that the rate of trap-assisted recombination is slower than band-to-band recombination. To further confirm this hypothesis, we have checked that the dynamics relative to the low energy part of the PL peak is slower than that relative to the high energy part of the PL peak, see Fig. S3(b).

To assess the electronic transport properties of germanane flake arrays, we constructed interdigitated electrodes using a conventional optical lithography method and drop-cast a dispersion of germanane flakes onto the electrodes. Figure 3(b) shows I-V characteristics of the germanane flake array at different temperatures. The arrays appear to be conductive, displaying decreasing conductance with decreasing temperature. Fitting the current-temperature curve to an Arrhenius law [Fig. 3(c)] allows for the extraction of an activation energy of 118 meV in the vicinity of room temperature. Because this activation energy is much smaller than one half of the bandgap—the expected value for intrinsic semiconductors—this suggests residual doping within the material. To determine the nature of this doping, we integrated the material in a field effect transistor. We use an ion gel electrolyte gating which has proven to be a viable approach for low gate bias field effect transistors made from colloidal nanocrystals³² and 2D materials,³³ as shown in the schematic in Fig. 3(a). This strategy has been particularly successful for achieving gating in thick, heterogeneous films while allowing stable operation in ambient air.³⁴ The transfer curve [Fig. 3(d)] reveals p-type character (i.e., a rise of conductance under hole injection at negative gate biases) for the methyl-terminated germanane flake arrays; this is consistent with previous observations obtained using a back gated geometry.²⁶ The on/off ratio of the transistor reached a factor of 250 over only $\pm 2 \text{ V}$ of gate bias operation. It is also worth pointing that the turn-on voltage of the transistor is around 100 mV , which is very similar to the activation energy determined from the I-T curve. This suggests that the Fermi level of the material lies in the vicinity ($100 \pm 20 \text{ meV}$) of the valence band.

Under illumination, arrays of methyl-terminated germanane flakes display a positive photoresponse (i.e., a rise in conductance under illumination), as shown in Fig. 4(a). The time response of the device is typically below $100 \text{ } \mu\text{s}$ with a weak temperature dependence. This corresponds in the frequency domain to a 3 dB cut-off frequency above 1 kHz , see Fig. 4(b). The power dependence of the photoresponse appears to present a power law dependency where the exponent is close to 0.5, as shown in Fig. 4(c). This suggests that the photocarrier lifetimes are limited by a bimolecular process^{35,36} (i.e., band-to-band

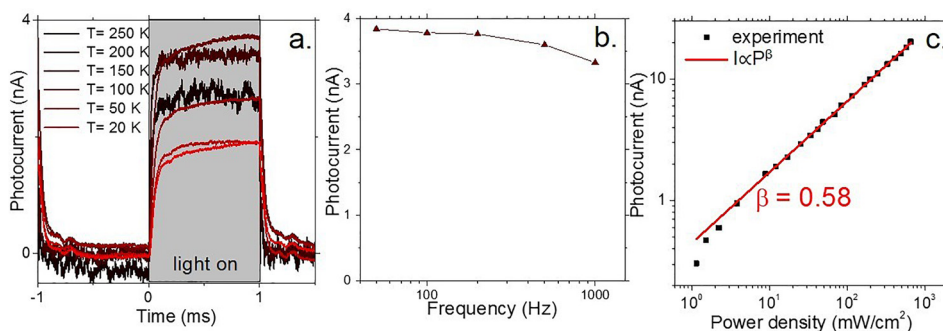


FIG. 4. (a) Current as a function of time, while the sample is illuminated by a pulse of light ($\lambda = 405 \text{ nm}$; $P \approx 2 \text{ mW}$), at different temperatures. The measurement is made under a +5 V bias. (b) Frequency dependence of the photocurrent, at room temperature. (c) Current as a function of light incident power. Measurements are obtained at room temperature under 5 V bias.

recombination), rather than by trapping. This observation is consistent with the absence of traps in the PL spectrum at room temperature.

In conclusion, we have investigated the photoluminescence and electronic transport properties of methyl-terminated germanane flakes. The PL signal of the flakes was found to have two contributions: one from the band edge and the other that is attributed to trap states. The PL linewidth is found to have a homogeneous origin and a carrier lifetime in the range of 1–100 ns. Arrays of methyl-terminated flakes exhibit p-type conduction. The material is also photoconductive with a fast time response of the order of 100 μ s, mostly limited by interband recombination.

See the [supplementary material](#) for information about material synthesis, material characterization, and additional transport measurements.

E.L. acknowledges the financial support of the European Research Council (ERC) starting grant (blackQD—No. 756225). We thank Agence Nationale de la Recherche for funding through grant Nanodose and IPER-nano2. This work was supported by French state funds managed by the ANR within the Investissements d'Avenir programme under Reference No. ANR-11-IDEX-0004-02 and more specifically within the framework of the Cluster of Excellence MATISSE. We acknowledge the use of clean-room facilities from the “Centrale de Proximité Paris-Centre.” This work was supported by the Region Ile-de-France in the framework of DIM Nano-K. This work was partially supported by the Air Force Office of Scientific Research Young Investigator Program (Grant No. FA9550-17-1-0170) and the National Science Foundation Early Career Development (CAREER) Award (Award No. 1847370). M.G.P. also acknowledges support from the Herbert L. Stiles Faculty Fellowship. B.J.R. acknowledges support from the National Science Foundation Graduate Research Fellowship under DGE No. 1744592.

The authors declare no competing financial interests.

REFERENCES

- ¹H. Chen, H. Liu, Z. Zhang, K. Hu, and X. Fang, *Adv. Mater.* **28**, 403 (2016).
- ²N. Goubet, A. Jagtap, C. Livache, B. Martinez, H. Portalès, X. Z. Xu, R. P. S. M. Lobo, B. Dubertret, and E. Lhuillier, *J. Am. Chem. Soc.* **140**, 5033 (2018).
- ³T. Erdem and H. V. Demir, *Color Science and Photometry for Lighting with LEDs and Semiconductor Nanocrystals* (Springer Singapore, 2019).
- ⁴B. Martinez, J. Ramade, C. Livache, N. Goubet, A. Chu, C. Greboval, J. Qu, W. Watkins, L. Becerra, E. Dandeu, J. L. Fave, C. Méthivier, E. Lacaze, and E. Lhuillier, *Adv. Opt. Mater.* **2019**, 1900348.
- ⁵E. Georgitzikis, P. E. Malinowski, L. M. Hagclsieb, V. Pejovic, G. Uytterhoeven, S. Guerrieri, A. Süss, C. Cavaco, K. Chatzinis, J. Maes, Z. Hens, P. Heremans, and D. Cheyns, in *2018 IEEE Sensors* (2018), pp. 1–4.
- ⁶B. T. Diroll, K. S. Schramke, P. Guo, U. R. Kortshagen, and R. D. Schaller, *Nano Lett.* **17**, 6409 (2017).
- ⁷L. Mangolini, E. Thimsen, and U. Kortshagen, *Nano Lett.* **5**, 655 (2005).
- ⁸X. Lu, B. A. Korgel, and K. P. Johnston, *Chem. Mater.* **17**, 6479 (2005).
- ⁹X. Lu, K. J. Ziegler, A. Ghezelbash, K. P. Johnston, and B. A. Korgel, *Nano Lett.* **4**, 969 (2004).
- ¹⁰P. Vogt, P. De Padova, C. Quaresima, J. Avila, E. Frantzeskakis, M. C. Asensio, A. Resta, B. Ealet, and G. Le Lay, *Phys. Rev. Lett.* **108**, 155501 (2012).
- ¹¹M. E. Dávila, L. Xian, S. Cahangirov, A. Rubio, and G. L. Lay, *New J. Phys.* **16**, 095002 (2014).
- ¹²W. Peng, T. Xu, P. Diener, L. Biadala, M. Berthe, X. Pi, Y. Borensztein, A. Curcella, R. Bernard, G. Prévot, and B. Grandidier, *ACS Nano* **12**, 4754 (2018).
- ¹³Z. Ni, Q. Liu, K. Tang, J. Zheng, J. Zhou, R. Qin, Z. Gao, D. Yu, and J. Lu, *Nano Lett.* **12**, 113 (2012).
- ¹⁴S. Jiang, M. Q. Arguilla, N. D. Cultrara, and J. E. Goldberger, *Chem. Mater.* **28**, 4735 (2016).
- ¹⁵S. Jiang, S. Butler, E. Bianco, O. D. Restrepo, W. Windl, and J. E. Goldberger, *Nat. Commun.* **5**, 3389 (2014).
- ¹⁶T. J. Asel, E. Yanchenko, X. Yang, S. Jiang, K. Krymowski, Y. Wang, A. Trout, D. W. McComb, W. Windl, J. E. Goldberger, and L. J. Brillson, *Appl. Phys. Lett.* **113**, 061110 (2018).
- ¹⁷Y. Ma, Y. Dai, W. Wei, B. Huang, and M.-H. Whangbo, *Sci. Rep.* **4**, 7297 (2014).
- ¹⁸Z. Liu, Z. Wang, Q. Sun, Y. Dai, and B. Huang, *Appl. Surf. Sci.* **467–468**, 881 (2019).
- ¹⁹G. Coloyan, N. D. Cultrara, A. Katre, J. Carrete, M. Heine, E. Ou, J. Kim, S. Jiang, L. Lindsay, N. Mingo, D. Broido, J. P. Heremans, J. Goldberger, and L. Shi, *Appl. Phys. Lett.* **109**, 131907 (2016).
- ²⁰N. D. Cultrara, Y. Wang, M. Q. Arguilla, M. R. Scudder, S. Jiang, W. Windl, S. Bobev, and J. E. Goldberger, *Chem. Mater.* **30**, 1335 (2018).
- ²¹E. Bianco, S. Butler, S. Jiang, O. D. Restrepo, W. Windl, and J. E. Goldberger, *ACS Nano* **7**, 4414 (2013).
- ²²R. K. Ghosh, M. Brahma, and S. Mahapatra, *IEEE Trans. Electron Devices* **61**, 2309 (2014).
- ²³H. Shu, Y. Li, S. Wang, and J. Wang, *J. Phys. Chem. C* **119**, 15526 (2015).
- ²⁴N. D. Cultrara, M. Q. Arguilla, S. Jiang, C. Sun, M. R. Scudder, R. D. Ross, and J. E. Goldberger, *Beilstein J. Nanotechnol.* **8**, 1642 (2017).
- ²⁵W. Amamou, P. M. Odenthal, E. J. Bushong, D. J. O'Hara, Y. K. Luo, J. van Baren, I. Pinchuk, Y. Wu, A. S. Ahmed, J. Katogh, M. W. Bockrath, H. W. K. Tom, J. E. Goldberger, and R. K. Kawakami, *2D Mater.* **2**, 035012 (2015).
- ²⁶B. N. Madhushankar, A. Kaverzin, T. Giousis, G. Potsi, D. Gournis, P. Rudolf, G. R. Blake, C. H. van der Wal, and B. J. van Wees, *2D Mater.* **4**, 021009 (2017).
- ²⁷N. G. Sahoo, R. J. Esteves, V. D. Punetha, D. Pestov, I. U. Arachchige, and J. T. McLeskey, *Appl. Phys. Lett.* **109**, 023507 (2016).
- ²⁸M. Q. Arguilla, N. D. Cultrara, M. R. Scudder, S. Jiang, R. D. Ross, and J. E. Goldberger, *J. Mater. Chem. C* **5**, 11259 (2017).
- ²⁹A. C. Serino, J. S. Ko, M. T. Yeung, J. J. Schwartz, C. B. Kang, S. H. Tolbert, R. B. Kaner, B. S. Dunn, and P. S. Weiss, *ACS Nano* **11**, 7995 (2017).
- ³⁰W. D. Kim, D. Kim, D.-E. Yoon, H. Lee, J. Lim, W. K. Bae, and D. C. Lee, *Chem. Mater.* **31**, 3066 (2019).
- ³¹N. M. Ravindra and V. K. Srivastava, *J. Phys. Chem. Solids* **40**, 791 (1979).
- ³²E. Izquierdo, A. Robin, S. Keuleyan, N. Lequeux, E. Lhuillier, and S. Ithurria, *J. Am. Chem. Soc.* **138**, 10496 (2016).
- ³³H. Henck, D. Pierucci, J. Chaste, C. H. Naylor, J. Avila, A. Balan, M. G. Silly, M. C. Asensio, F. Sirotti, A. T. C. Johnson, E. Lhuillier, and A. Ouerghi, *Appl. Phys. Lett.* **109**, 113103 (2016).
- ³⁴E. Lhuillier, S. Ithurria, A. Descamps-Mandine, T. Douillard, R. Castaing, X. Z. Xu, P.-L. Taberna, P. Simon, H. Aubin, and B. Dubertret, *J. Phys. Chem. C* **119**, 21795 (2015).
- ³⁵L. J. Willis, J. A. Fairfield, T. Dadosh, M. D. Fischbein, and M. Drndic, *Nano Lett.* **9**, 4191 (2009).
- ³⁶E. Lhuillier, J.-F. Dayen, D. O. Thomas, A. Robin, B. Doudin, and B. Dubertret, *Nano Lett.* **15**, 1736 (2015).